THE AMERICAN SOCIETY OF MECHANICAL ENGINEERS
Three Park Avenue, New York, N.Y. 10016-5990

99-GT-308

OPTICAL FIBRE AERODYNAMIC PROBES FOR TOTAL PRESSURE AND TOTAL TEMPERATURE MEASUREMENT IN TURBOMACHINERY

J. S. Barton, J. M. Kilpatrick, W. N. MacPherson, J. D. C. Jones,
Physics Department, Heriot-Watt University, Edinburgh EH14 4AS, UK

K. S. Chana, J. S. Anderson,
Propulsion Department, DERA Pyestock, Hampshire GU14 0LS, UK

D. R. Buttsworth* and T. V. Jones
Department of Engineering Science, Oxford University, Parks Road, Oxford OX1 3PJ, UK
*Current address: Faculty of Engineering and Surveying, University of Southern Queensland, Toowoomba 4350, Australia

ABSTRACT

Optical fibre sensors offer the prospect of miniature aerodynamic probes for highly localised flow measurements in aerospace wind tunnels and turbomachines. We discuss the design and construction of optical fibre sensors for temperature and pressure. The temperature sensors consist of multilayer coatings deposited on the fibre end face from which the reflected intensity is temperature-dependent. Two sensors were incorporated in a dual heated probe to measure total temperature. The pressure sensors are miniature diaphragms in which pressure-induced deflection is measured interferometrically in reflection. We present results from initial trials made in unsteady flow in a single stage research turbine, in which total temperature data with harmonic components up to 30 kHz and total pressure signals up to 230 kHz were recorded.

Nomenclature

- a diaphragm radius
- E Young's modulus
- h diaphragm thickness
- I optical intensity
- l sensor film thickness; sensor cavity length
- n refractive index
- P pressure
- q heat flux
- T temperature; $\overline{T}$ mean temperature
- V interference visibility
- ϕ optical phase
- λ light wavelength
- μ Poisson's ratio
- ρ density
- σ_m diaphragm maximum tensile stress

INTRODUCTION

Optical methods are familiar in aerodynamic research as techniques for non-intrusive localised and full-field measurements. For example, light scattering from seeding particles is employed in particle image velocimetry (Grant 1997) and in laser Doppler anemometry (Tropea 1995), and the reflected hue of liquid crystals is a measure of surface temperature (Wang et al., 1995). In contrast, this paper describes how an optical technique can be applied to point measurements made with aerodynamic probes by using optical fibres. Reflective sensors on the fibre ends are shown to be capable of measuring total temperature and pressure in transonic flow conditions. Optical fibres offer a potential reduction in transducer size, leading to smaller probes with improved spatial resolution, reduced blockage effects and the ability to probe flow passages with restricted access. An additional advantage of sensors connected by fibre only is their immunity from electromagnetic interference in comparison with electrical transducers.

The requirements for an ideal aerodynamic probe are small overall size, high bandwidth, high sensitivity to the desired measurand with zero sensitivity to other variables, and well-defined directional properties relative to the incident flow. All except the last of these requirements are determined primarily by the performance of the sensors. Electrical sensors are the basis for temperature and pressure measurement by probes in current usage, therefore we will briefly review the existing electrical transducers suitable for temperature and pressure probes.

Presented at the International Gas Turbine & Aeroengine Congress & Exhibition
Indianapolis, Indiana — June 7–June 10, 1999

Thermocouple junctions can be formed between small diameter wires, but their frequency response is limited by heat conduction in the supporting wires (Forney et al. 1993). A cold wire resistance thermometer was demonstrated by Dénos and Sieverding (1997) up to 6 kHz bandwidth by numerical compensation of the probe transfer function. Hot wires are unsatisfactory for unsteady flow temperature measurement as they respond to flow velocity and pressure fluctuations. The aspirating dual wire probe (Ng and Epstein 1983) avoids this difficulty by exposing two coplanar wires in a constant Mach number channel. Suryavamshi et al. (1998) have used such a probe to measure unsteady total temperature components up to 40 kHz in a multistage compressor.

The design of thin wire sensors is a compromise between the conflicting constraints on wire diameter to obtain high frequency response while retaining mechanical ruggedness in high speed flow. Wire-based sensors are susceptible to effects of contaminants in the flow, necessitating cleaning and recalibration. Some of these problems can be avoided by using thin film resistance gauges, developed for surface temperature measurements in heat flux studies, as temperature transducers. Buttsworth et al. (1998) describe a dual sensor probe for total temperature in which two thin film gauges are located at the stagnation points of quartz rods, operated at different temperatures. Total temperature measurements to an accuracy of ±1K with a bandwidth of 85 kHz, set by the heat transfer analogue circuit, were obtained in wind tunnel and turbine rig tests. In order to improve the spatial resolution, the technique has recently been modified to apply the two thin film gauges to the same quartz rod substrate, resulting in a probe less than 3mm diameter with the gauges separated by 0.7mm (Buttsworth and Jones 1998).

For pressure measurements in aerodynamic applications, the most highly developed transducers are electrical sensors comprising a silicon diaphragm with a piezoresistive bridge diffused into the upper surface. The output voltage results from pressure-induced strain in the diaphragm. A typical value for the lowest diaphragm resonant frequency might be 500 kHz with a sensor chip size about 1mm square. These sensors may be used in fast-response multi-hole probes to measure total pressure, flow speed and direction (Gossweiler et al. 1995) or embedded in blade models for surface pressure measurements on rotating blades (Ainsworth et al. 1991). The measurement bandwidth will depend on the presence of mechanical protection of the diaphragm, either by elastomer or by metal screening, and also on pneumatic cavity effects due to probe construction. Gossweiler et al. conclude that it is important to make probes as small as possible to minimise aerodynamic effects.

In this paper we describe novel total temperature and total pressure probes instrumented using optical fibre sensors. The temperature sensor is a multilayer coating developed from our previous single layer design (Kidd et al. 1995). The pressure sensor is a novel miniature diaphragm structure with optical read-out. Both sensors were shown to be capable of operating in transonic flow in a turbine test rig.

OPTICAL FIBRE SENSORS

Optical fibres are flexible dielectric waveguiding structures that offer the possibility for a wide range of fibre optic sensors. In this application, the advantages conferred by fibres are a small size measurement volume, immunity from electromagnetic interference, and a means of implementing optical interferometry as a high sensitivity technique in a difficult environment.

The optical fibre used in these experiments is a 3-layer coaxial cylinder structure. The inner core is typically 5 to 9 μm diameter, surrounded by a cladding 125 μm diameter, and an outer buffer layer 250 μm diameter. Core and cladding are conventionally fused silica, suitably doped to increase the core refractive index by ~0.5% relative to that of the cladding. Optical power launched into the fibre core is substantially confined within the core region by waveguiding. The buffer layer is a polymer coating which is added for mechanical protection, but can be easily removed if required. In use, fibres may be further protected by cable structures similar to their electrical counterparts and fibres can be bent to a radius of a few mm before there is any appreciable risk of breakage. Optical attenuation is low, typically 1 or 2 dB km^{-1}, so that fibre lengths of a few hundred metres do not impose significant power penalties. With a typical numerical aperture of 0.1, light leaves the exit face of the fibre over an angular range of ±6° to the fibre axis. Hence in conjunction with the small diameter of the core, a measurement region a few micrometres across at the fibre exit will be illuminated.

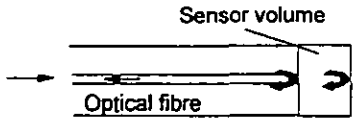

Figure 1 Generalised interferometric reflection sensor

There now exists a range of optical fibre sensors based on intensity modulation, light absorption, optical interferometry and polarisation techniques, e.g. as reviewed by Jackson (1994) and by Dakin and Culshaw (1997). We have chosen interferometry as the read-out method because of its sensitivity. An optical sensor within a probe is most conveniently used in reflection; the sensor is a reflective structure located on the fibre end, illuminated by core light coupled from the source (Fig. 1). Light reflected from the sensor can recouple into the same fibre and return to the optical system and detector. For interferometric sensing, light traversing the sensing volume reflects to combine, with phase difference ϕ, with the wave

initially reflected at the fibre end face. The resultant wave is an interference signal. In simplest case, two-beam interference results in a reflected intensity I which is a cosine function of the optical phase difference ϕ imposed by the sensor:

$$I = I_0(1+V\cos\phi) \quad (1)$$

where I_0 is the mean intensity and $0<V<1$ is the visibility of the interference which depends on the relative intensities and polarisation states of the interfering beams. The function of the sensor is to convert the applied measurand X to an optical phase change: $\phi = f(X)$. Hence the reflected intensity signal I can be related to X. In the application considered here X is gas temperature or pressure.

The temperature sensing element is a thin film of dielectric material on the fibre end; light is reflected from the front and rear faces of the film. The optical phase difference is sensitive to temperature due to the change in the refractive index of the film with temperature (the thermo-optic effect), with a smaller contribution from thermal expansion.

Pressure sensing is achieved by a small reflective diaphragm supported on the fibre end, leaving a small air cavity between the fibre and the diaphragm. Pressure-induced deflection of the diaphragm is detected by interferometric reflected signal from fibre end and diaphragm.

Each of these sensors will be considered in more detail below.

TEMPERATURE MEASUREMENT

Temperature sensor

The optical phase change in this case corresponds to the optical thickness of the sensor film, thickness l and refractive index n, traversed twice by light of wavelength λ:

$$\phi = \frac{4\pi nl}{\lambda} \quad (2)$$

If the mean temperature of the film changes by $\Delta\bar{T}$, the optical phase change is

$$\Delta\phi = \frac{4\pi l}{\lambda}\left[\frac{dn}{dT} + \frac{n}{l}\frac{dl}{dT}\right]\Delta\bar{T} \quad (3)$$

where the first term in the bracket represents the thermo-optic effect and the second is thermal expansion of the film. The sensor comprises 3 layers, metal-semiconductor-metal, applied to the fibre end in succession by vacuum evaporation (Fig. 2). The semiconductor chosen was zinc selenide; since it is relatively easy to deposit by thermal evaporation, and possesses a high thermo-optic coefficient dn/dT of 10^{-4}. We have previously shown that zinc selenide can be used as a single-layer sensor for temperature measurements in a multistage compressor (Kidd et al. 1995). The multilayer structure confers several advantages:

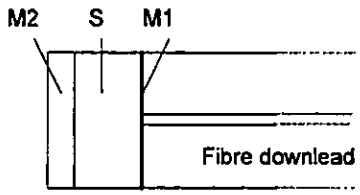

Figure 2 Temperature sensor schematic

the reflected signal power is increased; the visibility of interference can be high; and the outer metal coating protects the semiconductor film from contaminants such as dust or oil mist in the incident flow. Typical layer thicknesses were 10 nm nickel for the inner coating (M1 in Fig.2), 2 μm zinc selenide as the sensor film (S), and 100 nm aluminium as the outer coating (M2), sufficiently thick to protect the zinc selenide layer. With a thermal diffusion time of ~0.04 μs in response to a step change in temperature (Schultz and Jones 1973), the effect of the aluminium layer is not expected to be significant within the bandwidth of interest of ~100 kHz.

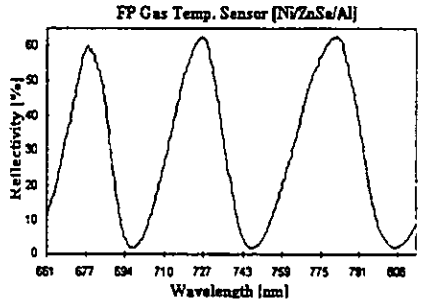

Figure 3 Wavelength scan of (Ni-ZnSe-Al) multilayer

The presence of the high reflectivity metal coatings will promote multiple reflections within the film, with the result that the simple two-beam transfer function of Eqn (1) will not apply. Modelling of the multiple reflections (Kilpatrick et al. 1997) shows that the transfer function's shape depends on the relative reflectivities and absorption of the metal coatings. The 10 nm nickel coating was chosen for its combination of reflectivity and absorption, together with the higher reflectivity 100 nm aluminium coating, to produce an asymmetric sawtooth dependence of reflected power versus phase. This is shown experimentally by the wavelength scan of a sensor at constant temperature in Fig. 3.

The optical system used to interrogate the sensor is shown in Fig. 4. A single wavelength is satisfactory as the expected phase changes for this application are relatively small. The laser diode wavelength (792 nm) was chosen to be close to mid-point of the steeper slope in Fig. 3. This affords maximum sensitivity to a small optical phase change arising from a sensor

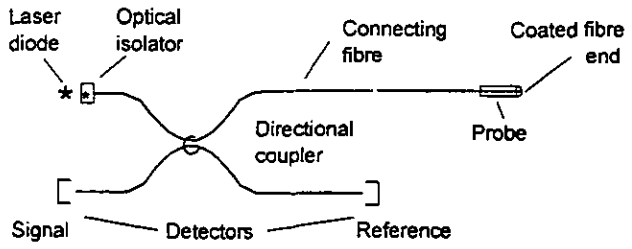

Figure 4 Optical system of the temperature sensor

temperature change with fixed wavelength illumination (eqn. (3)). For temperature changes < 150K the phase change is sufficiently small, <0.5 radians, for the transfer function to be reagrded as approximately linear. The temperature calibration is shown in Fig. 5: as the film temperature increases, the transfer function of Fig. 3 effectively moves slightly rightwards, resulting in a linear output signal from 20 to 120 °C. A noise floor (RMS) equivalent to a temperature amplitude of ~50 mK was typically observed in a 200 kHz measurement bandwidth in this temperature range.

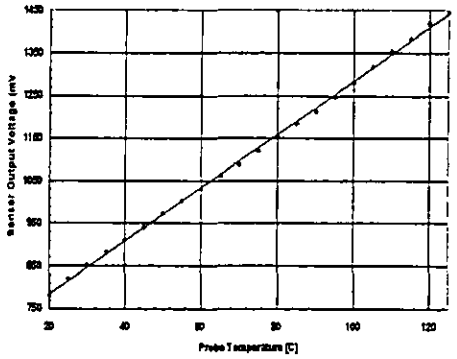

Figure 5 Multilayer sensor calibration, 20 to 120°C, using a laser diode wavelength of 792 nm

Total temperature probe

In order to measure gas total temperature, the dual probe design, originally using thin film resistance gauges (Buttsworth et al. 1998), was adopted. Measurements of heat flux to two aerodynamically similar probes at different surface temperatures enable the unknown heat transfer coefficient to be eliminated and gas total temperature found. Optical temperature sensors were axially embedded each within a 3 mm diameter cylindrical brass rod with a hemispherical end. Heating was applied to one sensor by passing current through a fine resistance wire wrapped around the fibre end. About 15 W heating power applied 20 s before a test-rig run was sufficient to generate a 50 K temperature difference between the hot and cold sensors within the probe. When exposed to a transient flow, the signals from both sensors, T_1 and T_2, provide surface temperatures from which the surface heat fluxes q_1, q_2 can be obtained numerically. With the assumption that the convective heat transfer coefficient h is the same at each sensor, the gas total temperature T_t is given by (Buttsworth et al. 1998)

$$T_t = T_1 + q_1(T_2 - T_1)/(q_1 - q_2) \qquad (4)$$

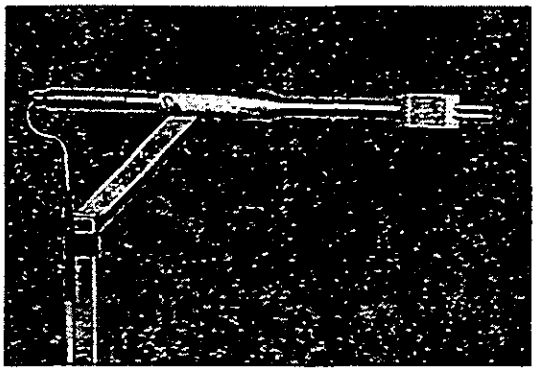

Figure 6 Total temperature probe: each brass rod (diam. 3mm) contains a multilayer coated optical fibre sensor

The total temperature probe is illustrated in Fig. 6, in which the probe mounting has been designed for use in the turbine test rig described below. Both optical fibres and the electrical supply to the sensor heater are contained in the small diameter stainless steel tube on the probe mounting. The connecting fibres were approximately 10 m in length, and were protected by standard 'fanout' tubing between the test rig and the control room where the optics and data acquisition systems were located.

PRESSURE MEASUREMENT

Pressure sensor

The principle of operation is the pressure-induced deformation of an elastic diaphragm fixed at a short distance from the end face of the optical fibre downlead used to address the sensor. The diaphragm and fibre end form an optical Fabry-Pérot cavity, and deformation of the diaphragm thus modulates the optical phase difference in the cavity. The cavity is sealed, and contains air at ambient atmospheric pressure. Sensors were constructed using a standard fibre connector (ST type) ferrule, fabricated from zirconia ceramic to support the fibre and diaphragm, which can be machined to reduce its outside diameter to ~800 μm. Such ferrules contain an axial hole that is closely toleranced to standard fibre dimensions; the addressing fibre was fixed in the ferrule by epoxy, slightly recessed from the end onto which the diaphragm is attached. The diaphragm was a 3μm copper foil, vacuum deposited onto a microscope slide with a gold release layer, and attached by epoxy to the

ferrule end. The cavity length was measured interferometrically, by analysis of the reflected spectrum from the sensor, and was found to be less than 20 μm for typical sensors. The structure is shown schematically in Fig. 7.

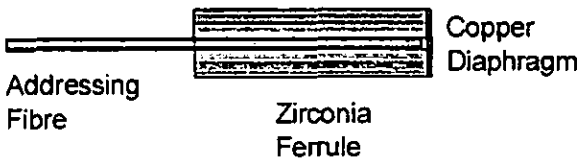

Figure 7 Pressure sensor schematic.

Since the diaphragm is non-transmissive, the sensor is optically isolated from the incident flow, preventing airborne contaminants affecting the reflected optical signal. The sensor was interrogated by an optical system similar to that shown in Fig. 4, in which the source was a 30mW, 780nm laser diode.

The response (Fig. 8) closely approximates the two-beam transfer function of Eqn. (1). Single wavelength interrogation was used for simplicity in initial experiments using an arrangement similar to that in Fig. 4; we have also used a dual wavelength scheme to compensate for signal variations due to common-mode effects such as fibre bending. We have previously described (MacPherson et al. 1997) a more general three-wavelength algorithm, applicable to this class of sensors, that is immune to additive and multiplicative noise and that does not require the assumption of a two-beam transfer function.

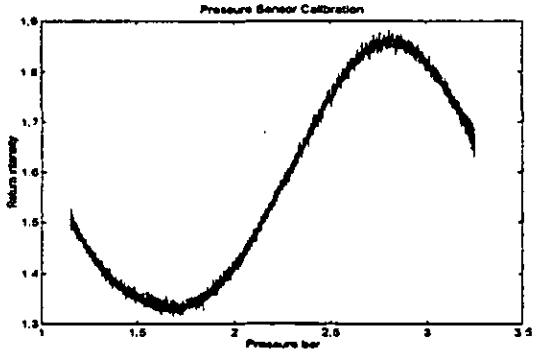

Figure 8 Reflected optical signal as a function of pressure

The performance of the sensor can be analysed using the standard equations describing a simply-supported circular diaphragm (Di Giovanni 1992). The relevant parameters are the bursting pressure P_m, the lowest resonant frequency f and the pressure sensitivity of the optical phase change, which are related to the mechanical properties and dimensions of the diaphragm as follows:

$$P_m = \sigma_m \frac{8}{3(1+\mu)} \frac{h^2}{a^2} \tag{5}$$

$$f = \frac{10.21}{2\pi a^2}\sqrt{\frac{D}{h\rho}} \quad \text{where } D = \frac{Eh^3}{12(1-\mu^2)} \tag{6}$$

$$\frac{\Delta\phi}{\Delta P} = \frac{\Delta\phi}{\Delta l}\frac{\Delta l}{\Delta P} = \frac{4\pi n}{\lambda}\frac{3(1-\mu^2)a^4}{16Eh^3} \tag{7}$$

Eqn. (7) follows from the diaphragm deflection sensitivity applied to Eqn. (2). The observed pressure sensitivity was typically 2.9 rad bar^{-1}, which corresponds to a diaphragm thickness h = 2.2μm, for a copper diaphragm of radius a = 62.5 μm. The observed pressure resolution was ~5mb which is equivalent to a 1 nm diaphragm deflection, and the sensor's operating range covered vacuum to 5 bar absolute pressure. From Eqn. (6), the expected resonant frequency was 1.1 MHz.

The construction as described will be sensitive to temperature change, in that the zirconia ferrule has a thermal expansion coefficient of 8×10^{-6}, which yields a temperature sensitivity for a 16 μm cavity of approximately 2 mrad K^{-1}, equivalent to an apparent pressure change of 0.7 mb K^{-1}. Note that the temperature sensitivity scales with sensor cavity length, while the pressure sensitivity (Eqn.(7)) is independent of length. The measured temperature sensitivity was 35 mb K^{-1}, which is significantly larger that the estimate based on thermal expansion of the zirconia ferrule, but is consistent with our estimates of contributions from other possible thermal sensitivities, including expansion of the adhesive, a longer effective length of ferrule unsupported by epoxy, pressure increase of the air within the cavity, and thermally-induced diaphragm distortion. Several measures may be taken to reduce thermal sensitivity: a shorter cavity will reduce the temperature cross sensitivity, without affecting the pressure sensitivity; forming the cavity under vacuum, rather than at atmospheric pressure would eliminate pressure effects in the cavity air; and finally, improvements in diaphragm construction, for example pre-tensioning the diaphragm to reduce buckling.

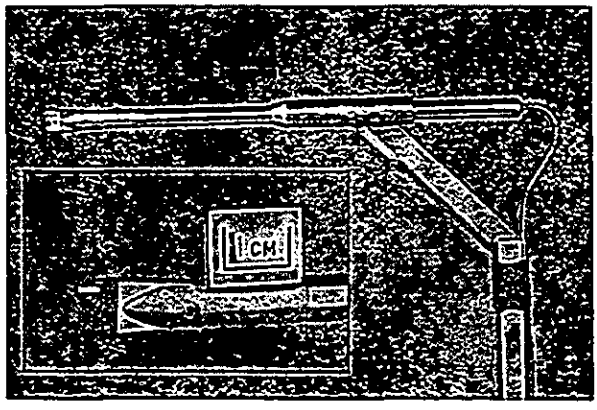

Figure 9 Wedge probe for turbine tests: (inset) probe head with optical fibre sensor in total pressure position

Total pressure probe

An optical pressure sensor was incorporated in a wedge probe as a total pressure sensor, within a stainless steel capillary tube 1.6mm outside diameter, facing into the flow. The diaphragm was not screened. The wedge was 6.6 mm in height and 5 mm in depth measured along the wedge face in the flow direction. The probe, illustrated in Fig. 9, was mounted on a stem in a similar fashion to the total temperature probe.

AERODYNAMIC TESTS

Shock tube tests

Before being run in the turbine test rig, the sensors were compared with their electrical counterparts in a small scale shock tube. This consisted of two 1m lengths of steel pipe of 25 mm inside diameter with a Mylar burst-diaphragm between them. The driver section was slowly pressurised with nitrogen gas until the diaphragm burst, initiating a shock wave to propagate towards the sensor situated in the working section. With a burst pressure of ~3 bar, the initial wavefront introduces a step increase of pressure of approximately 1 bar.

The purpose of the shock tube experiments was to verify the calibrations of the sensors in a dynamic test and to examine their behaviour in transient flow before installing them in the turbine test rig. The dual temperature probe was installed in the shock tube's end section facing forward. For these comparison trials, it was instrumented with one optical fibre multilayer temperature sensor and one thin film Pt resistance gauge, 2 × 1mm, each exposed on 3 mm tip diameter rods of brass and quartz respectively.

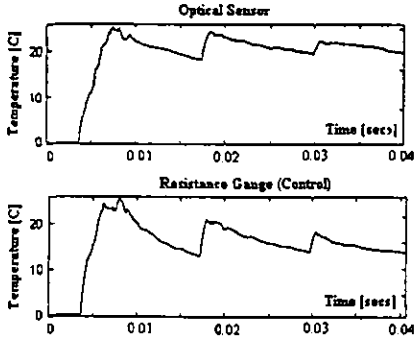

Figure 10 Shock tube test of (upper) optical temperature sensor compared with (lower) Pt thin film gauge in forward-facing total temperature probe

Data were captured at 200 ksample s^{-1}, initiated by the signal from a piezoelectric pressure sensor located in the sidewall upstream of the temperature probe. The optical and electrical sensor temperature-time signals are shown in Fig. 10. A rapid rise of approximately 25 K occurs at the incident shock, repeated successively at ~ 10 ms intervals by the shock reflection from the far end of the tube. In order to test the optical sensor's ability to survive exposure to transient flow, 24 repeated shock tests were made on the same probe, for which consistent results were obtained.

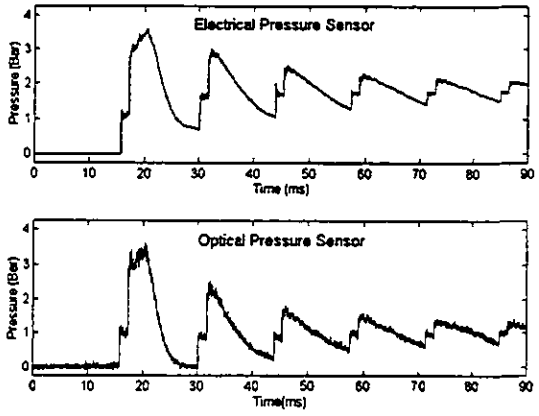

Figure 11 Shock tube pressure-time signals (upper) electrical sensor; (lower) optical sensor

The optical pressure sensor was similarly compared with a high bandwidth silicon diaphragm sensor. For these tests, the sensors were exposed in the sidewall of the test section, mounted flush with the internal surface. Pressure-time signals are shown in Fig. 11. We attribute the slightly larger amplitude of the reflected shock signals to thermal effects in the optical gauge. The RMS noise levels for the electrical and optical pressure sensors were 4 mb and 36 mb respectively. The noise in the optical sensor was reduced to 5 mb RMS in the turbine tests described below by tuning the laser diode source to a more stable operating point.

In addition, the resonant frequency of the pressure sensor diaphragm was observed as follows. The sensor was installed flush with the end plate of the shock tube, facing into the flow. Data were captured at 100 Msamples s^{-1} for a 1 ms interval at the incident shock. The spectrum of a 150 μs sample of the sensor signal immediately after the pressure step (Fig. 12) shows a clear resonant peak frequency at 1.017 MHz.

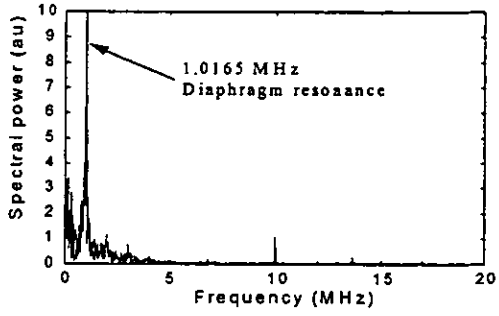

Figure 12 Spectrum of optical pressure sensor signal exposed to impulsive pressure step in shock tube

Turbine rig tests

The Isentropic Light Piston Facility (DERA Pyestock, Farnborough, UK) is a transient flow facility for turbomachinery research designed to simulate engine conditions in a single turbine stage. The working section, approximately 1m in diameter, contains a circumferential ring of nozzle guide vanes upstream of the rotor. Sensors are typically mounted on the casing, on the blades, or in probes several millimeters downstream of the rotor stage as in this experiment. The rotor is spun up to speed, typically 9,500 rpm, prior to the run start with the working section initially evacuated. A piston is driven by high pressure air along a pump tube, adiabatically compressing the air ahead if it, until a fast-acting valve opens to admit the flow to the working section, a turbobrake and finally a large dump tank. The run duration, in which operating conditions were steady, was approximately 600 ms. In the tests described here, the resulting transonic flow was measured by probes mounted several mm downstream from the rotor stage facing directly into the average flow.

Total temperature results

The sensor temperatures were recovered by taking the reflected optical signal from each, divided by the reference signal to remove fluctuations in laser diode output power, and applying the appropriate calibration data as shown in Fig.5. An initial run was made with no heating applied to the 'hot' sensor, to check consistency between the two sensors. The observed difference was less than 0.5 K over most of the 600 ms run time, in which the probe tips heated from ambient (~20 °C) to approximately 50 °C.

To measure total temperature, heating was applied prior to the start of the run. The hot sensor was typically at 70°C and the cold sensor at 25°C at the onset of the flow through the working section.

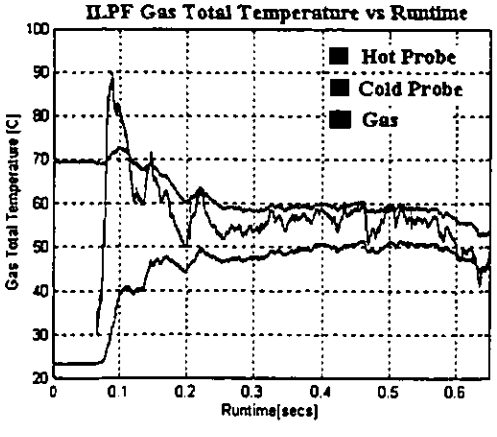

Figure 13 Dual sensor temperatures in ILPF turbine test: upper trace – hot sensor; lower trace – cold sensor; central trace – derived gas total temperature

Temperature-time signals are shown in Fig. 13, indicating the expected convergence of both sensor temperatures to the mean gas temperature. Each sensor temperature was processed by a finite difference method (Buttsworth et al. 1998) to yield the surface heat fluxes q_1 and q_2 , from which the time-dependent gas total temperature was evaluated using Eqn. (4). Before the onset of the flow, the temperature signals in Fig.13 show ~ 50 mK RMS noise in a 200 kHz measurement bandwidth. Closer examination of the total temperature data during the flow reveals gas temperature oscillations of ~6 K amplitude at blade passing frequency (9.5 kHz), for which the sensor signal amplitude was typically 200 mK. The power spectrum of data averaged over 40 rotations is shown in Fig. 14, in which harmonics are present up to ~30 kHz.

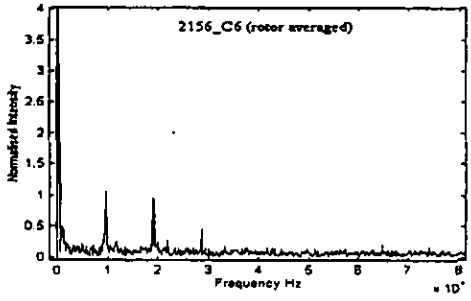

Figure 14 Spectrum of rotor-averaged total temperature data from optical probe, blade passing frequency 9.5 kHz

Total pressure results

As the flow became established in the ILPF, the pressure rise in the working section was sufficient to drive the interferometer signal over one minimum and one maximum of the transfer function shown in Fig. 8. The corresponding pressure change of 1.68 bar, reached ~200 ms after the flow onset, was in good agreement with that measured by a comparison electrical sensor. This suggests that the temperature cross-sensitivity is not producing a significant pressure error in the timescale of the transient flow experiment. The pre-run data, with the working section evacuated and the rotor at design speed just prior to the onset of flow, show an RMS noise of 5 mb. There is no component at blade passing frequency, indicating that the sensor and its connecting fibre are not exhibiting vibrational sensitivity.

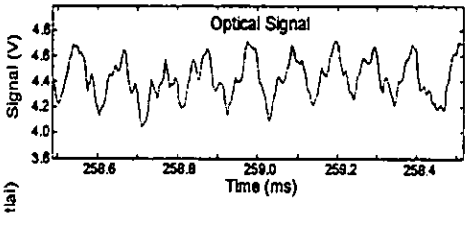

Figure 15 Optical pressure sensor signal during ILPF run time

The flow regime of interest was established in the working section for a duration of ~ 350 ms. A typical portion of the optical sensor signal is shown in Fig. 15. These data are processed essentially by a cosine fit to the transfer function, from which the optical phase, and hence the pressure change, is derived. Pressure signals averaged over 40 revolutions (Fig. 16) show clear structure with a single peak plus one or two side lobes per blade. The power spectrum of rotor-averaged data (Fig. 17) contains a series of harmonics of blade passing frequency (9.5 kHz) up to ~230 kHz on a smoothly decreasing noise background.

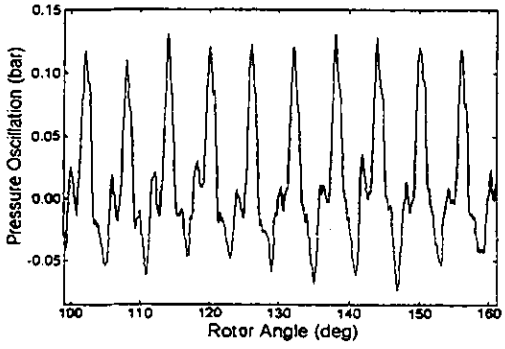

Figure 16 Rotor-averaged pressure data

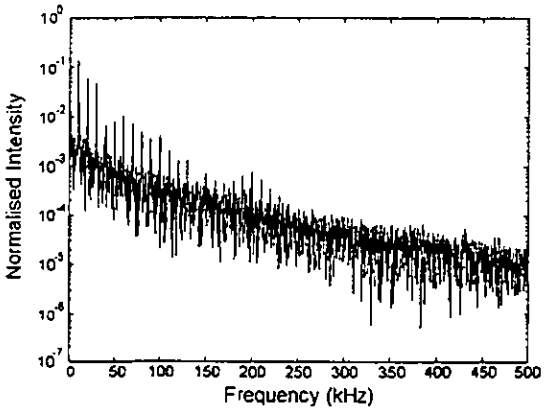

Figure 17 Power spectrum of rotor-averaged pressure data

DISCUSSION AND CONCLUSIONS

We have described the application of optical fibre sensors to total temperature and total pressure measurement. The sensors are based on optical interferometry and are electrically passive, interrogated by a single fibre connecting the probe to the optical source and detection system. In particular, fibres confer the advantage of a very small sensing volume, of the order of the fibre core diameter of ~5 μm within a sensor structure located on the fibre end. The temperature sensors were multilayer coatings and the pressure sensors were ceramic ferrules capped by a metal diaphragm.

The sensors have been integrated into aerodynamic probes and demonstrated downstream of the rotor in a full-scale transient turbine test facility. Both temperature and pressure probes continued to function without significant change in calibration after 8 runs in the turbine test rig. Total temperature has been measured using a dual sensor probe with a resolution of ~1 K in a 200 kHz measurement bandwidth, showing signal components up to 30 kHz. This bandwidth is smaller than that of the Pt thin film dual temperature probe, but is comparable to the dual hot-wire probe with the potential for easier miniaturisation. The optical sensor's bandwidth may be improved by employing silicon rather than zinc selenide as the central element of the multilayer coating. Compared with zinc selenide, silicon offers a factor of 12 increase in thermal diffusivity and 2 in thermo-optic coefficient. Preliminary tests with single layer silicon coatings have confirmed an increase in performance.

Total pressure has been measured in the same test rig at a resolution of 5μb $Hz^{-0.5}$ with a diaphragm resonant frequency of 1 MHz, showing signal components up to 230 kHz. Thus the performance compares favourably with a piezo-resistive gauge with similar operating range of ~7 bar, which exhibits a first resonant frequency of ~650kHz and a measured noise floor of ~3μb $Hz^{-0.5}$. The optical sensor is 800 μm in diameter with a sensing area defined by the unsupported diaphragm area 125 μm in diameter.

The objective of this work was primarily to demonstrate the potential of fibre sensors as transducers in aerodynamic probes. The probes used were existing designs, and were not miniaturised. For future work, we will investigate alternative diaphragm materials and support structures to reduce further the size of the pressure sensor, and integrate smaller sensors into multihole pressure probes of higher spatial resolution.

Acknowledgements

This work is supported by the UK Engineering and Physical Sciences Research Council, whom W. N. MacPherson acknowledges for the provision of a studentship.

REFERENCES

Ainsworth R. W., Dietz A. J., Nunn T. A., 1991, 'The use of semi-conductor sensors for blade surface pressure measurement in a model turbine stage,' *Trans. ASME J. of Eng. for Gas Turbines & Power*, **113**, 261 - 268

Buttsworth, D. R., and Jones, T. V., 1998, "A Fast-Response High Spatial Resolution Total Temperature Probe Using a Pulsed Heating Technique," Trans. ASME Journal of Turbomachinery, Vol. 120, pp 601-607

Buttsworth, D. R., Jones, T. V. and Chana, K. S., 1998, "Unsteady Total Temperature Measurements Downstream of a High Pressure Turbine," Trans. ASME Journal of Turbomachinery, Vol. 120, pp. 760 - 767

Dakin J. and Culshaw B. (editors), 1997, *Optical Fiber Sensors vol IV,* Artech House, Boston & London

Dénos R. and Sieverding C.H., 1997, "Assessment of the Cold-Wire Resistance Thermometer for High-Speed Turbomachinery Applications", Trans. ASME J. of Turbomachinery, Vol. 119, pp. 140-148

Di Giovanni M., *Flat and Corrugated Diaphragm Design Handbook*, Marcel Dekker Inc, 1992

Forney L.J., Meeks E. L., Ma J., and Fralick G.C., 1993, "Measurement of Frequency Response in Short Thermocouple Wires," Review Sci. Instrum., Vol. 64, pp. 1280-1286

Gossweiler C.R., Kupferschmied P., and Gyarmathy G., 1995, "On fast-response probes: Part 1–Technology, calibration, and application to turbomachinery; Part 2–Aerodynamic probe design studies," Trans. ASME J. of Turbomachinery, Vol. 117, pp. 611-624

Grant I., 1997, "Particle Image Velocimetry: A Review," Proceedings of the Institution of Mechanical Engineers part C: Journal of Mechanical Engineering Science, Vol.211, pp.55-76

Jackson D.A., 1994, "Recent Progress in Monomode Fibre-Optic Sensors," Meas. Sci. Technol., Vol. 5, pp. 621-638

Kidd S.R., Barton J.S., Meredith P., Jones J.D.C., Cherrett M.A. and Chana K.S., 1995, "A fibre optic probe for gas total temperature measurement in turbomachinery," Trans. ASME J. of Turbomachinery Vol. 117, pp. 635 - 641

Kilpatrick J.M., MacPherson W.N., Barton J.S. and Jones J.D.C., 1997, "Reflection transfer Characteristics of an Optical Fibre Fabry-Perot Interferometer" *Sensors and their Applications VIII*, Augousti A.T. and White N.M. (eds), pp. 263-268, IOP Publishing, Bristol and Philadelphia

MacPherson W.N., Kidd S.R., Barton J.S. and Jones J.D.C., 1997, "Phase demodulation in optical fibre Fabry-Pérot sensors with inexact phase steps," IEE Proc. Optoelectronics, Vol.144, pp. 130-133

Ng W.F. and Epstein A.H., 1983, "High-Frequency Temperature and Pressure Probe for Unsteady Compressible Flows," Review Sci. Instrum., Vol. 54, pp. 1678-1683

Schultz D.L. and Jones T.V., 1973, "Heat Transfer Measurements in Short Duration Hypersonic Facilities," AGARD Report AG 165

Suryavamshi N., Lakshminarayana B., and Prato J., 1998, "Aspirating Probe Measurements of the Unsteady Total Temperature Field Downstream of an Embedded Stator in a Multistage Axial Flow Compressor", Trans. ASME Journal of Turbomachinery, Vol. 120, pp. 156-169

Tropea C., 1995, "Laser Doppler Anemometry: Recent Developments and Future Challenges," Meas. Sci. Technol., Vol. 6, pp. 605-619

Wang Z., Ireland P.T. and Jones T.V., 1995, "An Advanced Method of Processing Liquid Crystal Video Signals From Transient Heat Transfer Experiemnts", Trans. ASME Journal of Turbomachinery, Vol. 117, pp. 184-189